Our aim is to characterize the type of unmodeled dynamics Δ for which GAS of (1) is preserved by backstepping. Our results will specify a *stability margin* of (1), that is, an admissible region for the Nyquist plot of Δ.

In the backstepping technique a globally stabilizing virtual control $y = \alpha_0(x)$ for the x-subsystem is "backstepped" through the n integrators $y^{(n)}$ to compute the actual control u. There are several degrees of freedom in this procedure, starting with the choice of α_0. Under Assumption 1 we will take α_0 to be the *nonlinear damping*

$$\alpha_0(x) = -kL_gV(x), \quad k > \max(\rho, 0), \tag{3}$$

also referred to as Jurdjevic-Quinn control (Jurdjevic & Quinn 1978).

Assumption 2. The system $\dot{x} = f(x)$ with output $L_gV(x)$ is zero-state detectable, that is $L_gV(x(t)) \equiv 0$, $\forall t \implies \lim_{t\to\infty} x(t) = 0$. ◦

With $y = \alpha_0(x)$ in (1), we have

$$\dot{V} = \frac{\partial V}{\partial x}[f(x) + g(x)\alpha_0(x)] \le -(k-\rho)[L_gV(x)]^2,$$

which shows GAS of $\dot{x} = f(x) + g(x)\alpha_0(x)$ if Assumptions 1 and 2 are satisfied. (Assumption 2 can be waived if $\dot{x} = f(x)$ is GAS.)

We consider the two main versions of backstepping.

Backstepping with Cancelation.

Here the negativity of the derivative of the Lyapunov function at each step is achieved by *canceling* the sign-indefinite terms. In this case, the sequence of virtual controls $\alpha_1, \dots, \alpha_n$, with $\alpha_n = u$, is

$$\begin{aligned}
\alpha_1 &= -c_1(y-\alpha_0) - \mu LgV + \dot{\alpha}_0, & (4)\\
\alpha_2 &= -c_2(\dot{y}-\alpha_1) - (y-\alpha_0) + \dot{\alpha}_1, &\\
&\vdots &\\
\alpha_n &= u = -c_n(y^{(n-1)} - \alpha_{n-1}) - (y^{(n-2)} - \alpha_{n-2}) + \dot{\alpha}_{n-1}, & (5)
\end{aligned}$$

where $\mu, c_1, \dots, c_n$ are positive design parameters. In the nominal design $y^{(n)} = u$, and the derivative of the Lyapunov function

$$W(x, y-\alpha_0, \dots, y^{(n-1)} - \alpha_{n-1}) = V(x) + \frac{1}{2\mu}(y-\alpha_0)^2 + \dots + \frac{1}{2}(y^{(n-1)} - \alpha_{n-1})^2 \tag{6}$$

along the trajectories of (1), (5) is negative definite:

$$\dot{W} \le -(k-\rho)(L_gV)^2 - c_1(y-\alpha_0)^2 - \dots - c_n(y^{(n-1)} - \alpha_{n-1})^2. \tag{7}$$

Hence (1), (5) is GAS (Krstić, Kanellakopoulos & Kokotović 1995).

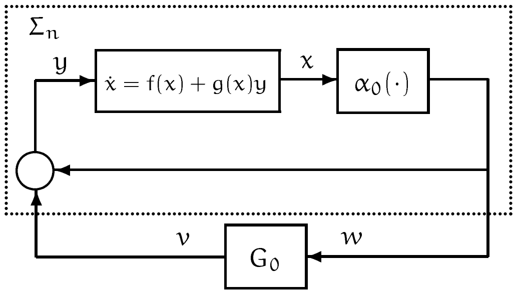

Figure 1: Controlled x-subsystem with input unmodeled dynamics.

Theorem 2.1 (Stability Margin of the x-Subsystem). Under Assumptions 1 and 2, the closed-loop system of Figure 1 with $\alpha_0(x) = -kL_gV(x)$ is GAS for all stable G_0 satisfying

$$\mathrm{Re}G_0(j\omega) > -1 + \frac{\rho}{k}. \tag{14}$$

Proof. The derivative of kV along the trajectories of the nominal system Σ_n is

$$\begin{aligned} k\dot{V} &= kL_fV(x) + kL_gV(x)[\nu - kL_gV(x)], \\ &\leq -k(k-\rho)[L_gV(x)]^2 + k\nu L_gV(x), \\ &= -\frac{k-\rho}{k}w^2 + \nu(-w), \end{aligned} \tag{15}$$

where $w = -kL_gV(x)$ and $\nu = G_0 w$, see Figure 1. We recognize in (15) the dissipation inequality corresponding to OFP $(1 - \rho/k)$, that is output feedback passivity with excess $1-\rho/k$ (in the terminology of Sepulchre, Janković & Kokotović (1997)) and storage function kV. The result follows from Theorem 2.34 in Sepulchre, Janković & Kokotović (1997). □

Since $\Delta = 1 + G_0$, the controlled x-subsystem preserves GAS with stable input unmodeled dynamics Δ whose Nyquist plot belongs to the half-plane $\mathrm{Re}\Delta(j\omega) > \frac{\rho}{k}$. We consider three cases:

Case $\rho > 0$. The stability margin is a half-plane strictly contained in the open right half plane, thus only biproper Δ's can be tolerated. As k increases, the half-plane plane moves to the left; hence, for larger nonlinear damping the stability margin is larger.

Case $\rho = 0$. The stability margin is the open right half plane, thus only biproper Δ's can be tolerated. The margin is unaffected by k.

Case $\rho < 0$. The stability margin includes the imaginary axis, thus allowing for strictly proper Δ's. As k increases, the half-plane moves to the right, which shows that for more aggressive nonlinear damping (larger k) the stability margin is smaller.

In the next sections we will explore how the stability margin is affected when one or more steps of backstepping are introduced.

-1. Figures 3 and 4 show, respectively, the Nyquist plots of biproper and strictly proper Δ's, and the corresponding G_1's for three values of c_1. The larger values of c_1 lead to plots covering a larger area of the complex plane. Moreover, if Δ has relative degree larger than two, then there is a maximum value of c_1 such that G_1 is stable. This is because the stability of G_1 is equivalent to the stability of the feedback interconnection of Δ and c_1/s.

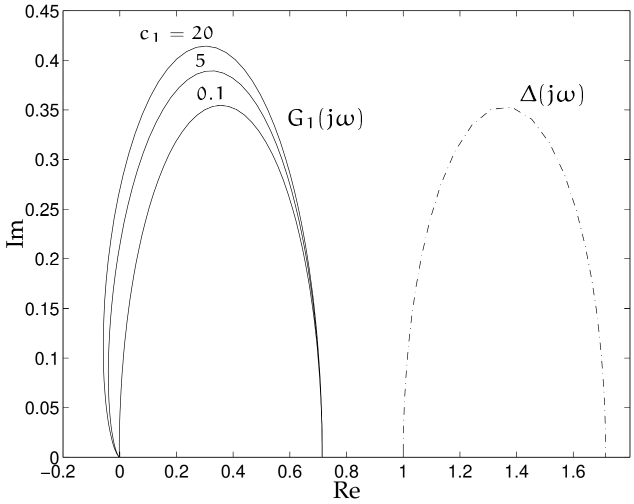

Figure 3: Nyquist plot of $\Delta(s) = \frac{12(s+35)(s+20)}{7(s+40)(s+30)}$ and equivalent G_1 for three values of c_1.

The nominal feedback system Σ_n, which corresponds to $G_1(s) = 0$ ($\Delta(s) = 1$), is GAS. The following theorem gives a class of G_1's (in turn, a class of Δ's) for which the closed-loop system in Figure 2 remains GAS after one step of backstepping.

Theorem 3.1 (Stability Margin of One Integrator Backstepping). Under Assumptions 1 and 2, the closed-loop system of Figure 2 with G_1 and F_1 given in (18) and nonlinear damping α_0 given in (3), is GAS for all stable $G_1(j\omega)$ satisfying

$$\left| G_1(j\omega) + \frac{S}{Q} \right|^2 < \frac{S^2}{Q^2} - \frac{R}{Q}, \tag{20}$$

or, equivalently

$$\begin{bmatrix} G_1(j\omega) \\ 1 \end{bmatrix}^* \begin{bmatrix} Q & S \\ S & R \end{bmatrix} \begin{bmatrix} G_1(j\omega) \\ 1 \end{bmatrix} < 0, \tag{21}$$

where

$$Q > 1, \qquad S = -2\frac{c_1}{\mu}k, \qquad R = -4\frac{c_1}{\mu}(k - \rho). \tag{22}$$

Proof. Let the realization of F_1 in (18), with input $\mu L_g V$, be

$$\dot{\xi}_1 = -c_1 \xi_1 + \mu L_g V(x), \tag{23}$$

with $1/(2\delta) = k^2 c_1/\mu + k - \rho$. Multiplying both sides of (26) by $2/\delta$, and rearranging, we get

$$\frac{2}{\delta}\dot{W} \leq v^2 - 4\frac{c_1}{\mu}k\,vw - 4\frac{c_1}{\mu}(k-\rho)\,w^2\,,$$

and, using (22), we obtain

$$\frac{2}{\delta}\dot{W} \leq v^2 + 2Svw + Rw^2\,. \tag{27}$$

Next, let G_1, with minimal state-space representation

$$\begin{aligned} \dot{z} &= Az + Bw \\ v &= Cz + Dw\,, \end{aligned} \tag{28}$$

satisfy (21). By the Kalman-Yakubovich-Popov Lemma there exists $P = P^T > 0$ such that

$$\begin{bmatrix} PA + A^T P + C^T QC & PB + C^T S \\ B^T P + S^T C & R \end{bmatrix} < 0\,. \tag{29}$$

Taking $U(z) = z^T P z$ as a storage function for (28) and using (29), we obtain

$$\dot{U} < -Qv^2 - 2Svw - Rw^2\,. \tag{30}$$

With $\frac{2}{\delta}W(x,\xi_1) + U(z)$ as a Lyapunov function for the feedback interconnection of Figure 2, it follows, from (27) and (30), that

$$\frac{2}{\delta}\dot{W} + \dot{U} < -(Q-1)v^2\,. \tag{31}$$

Since $Q > 1$ the equilibrium $(x, \xi_1, z) = (0, 0, 0)$ is globally stable. GAS is shown as in the proof of Theorem 2.33 in Sepulchre, Janković & Kokotović (1997), because, under Assumption 2, Σ_n is GAS when $v = 0$ and G_1 is stable. □

The dissipation inequality (30) corresponds to the property of *dissipativity* with *suply rate* $-(Qv^2 + 2Svw + Rw^2)$, introduced by Willems (1972) and Hill & Moylan (1976). In the form of inequality (21), it is used by Megretski & Rantzer (1997) in stability analysis with integral quadratic constraints.

Theorem 3.1 shows that GAS is preserved for stable G_1 of the form (18) whose Nyquist plot is in the disk shown in Figure 5. We are interested in analyzing the cases where this disk encircles the point -1 because, as discussed before, this implies that GAS is preserved under strictly proper unmodeled dynamics. We denote the difference between the radius and the center of the disk by

$$\begin{aligned} \sigma &= \sqrt{\frac{S^2}{Q^2} - \frac{R}{Q}} + \frac{S}{Q}\,, \\ &= \sqrt{a^2k^2 + 2a(k-\rho)} - ak\,, \end{aligned} \tag{32}$$

where we have used (22) and $a = \frac{2c_1}{Q\mu}$. We consider the following two cases.

Now we have

$$F_n(s) \triangleq \frac{N_{F_n(s)}}{D_{F_n(s)}} = \cfrac{1}{s + c_1 + \cfrac{1}{s + c_2 + \cdots + \cfrac{1}{s + c_{n-1} + \cfrac{1}{s + c_n}}}}, \tag{35}$$

$$G_n(s) \triangleq \frac{s^n[\Delta(s) - 1]}{\Delta(s) D_{F_n(s)} - s^n[\Delta(s) - 1]} \,. \tag{36}$$

With these new definitions for G_n and F_n, the closed-loop system (1), (5), can again be expressed as (19) (with G_n, F_n replacing G_1, F_1) and depicted as in Figure 2. The filter F_n in (35), whose block diagram is shown in Figure 6, is output feedback passive with excess c_1.

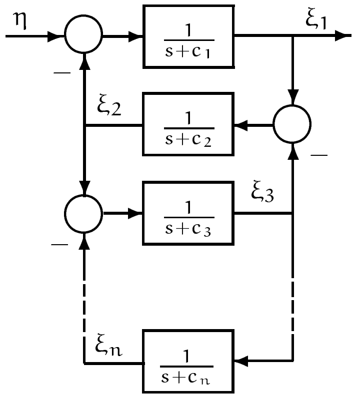

Figure 6: Filter F_n.

Lemma 3.2 (F_n is OFP(c_1)). Let $\bar{V}(\xi) = \frac{1}{2}\xi^T\xi$, where $\xi = [\xi_1, \xi_2, \ldots, \xi_n]$ is the state of the realization of F_n given in Figure 6. Then F_n satisfies the following dissipation inequality

$$\dot{\bar{V}} \le -c_1\xi_1^2 + \xi_1\eta \,. \tag{37}$$

Proof. For the filter state-space equation

$$\dot{\xi} = \begin{bmatrix} -c_1 & -1 & 0 & \ldots & 0 \\ 1 & -c_2 & -1 & \ldots & 0 \\ 0 & 1 & -c_3 & \ldots & 0 \\ & & & \ddots & \\ 0 & 0 & \ldots & 1 & c_n \end{bmatrix} \xi + \begin{bmatrix} 1 \\ 0 \\ 0 \\ \vdots \\ 0 \end{bmatrix} \eta \,, \tag{38}$$

the derivative of $\bar{V}(\xi)$ is

$$\dot{\bar{V}} = -c_1\xi_1^2 - c_2\xi_2^2 - \cdots - c_n\xi_n^2 + \xi_1\eta \le -c_1\xi_1^2 + \xi_1\eta \,,$$

which proves (37). □

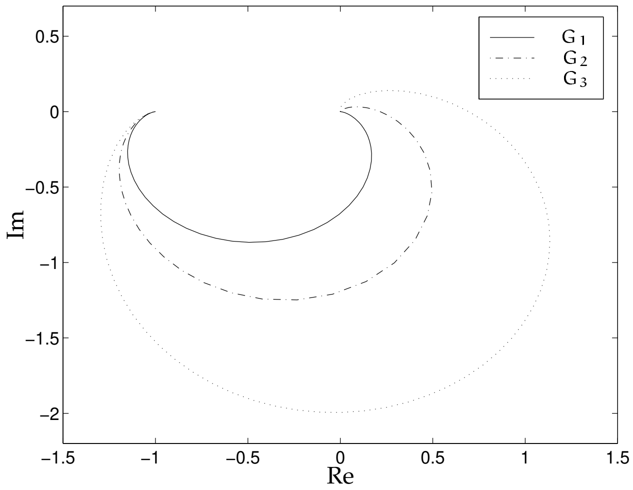

Figure 8: Nyquist plot of G_1, G_2 and G_3 for $\Delta(s) = \frac{1200}{(s+40)(s+30)}$ with $c_1 = c_2 = c_3 = 5$.

4 Backstepping with Domination

By taking the Laplace transform of the y-equation of (1), (9), we obtain

$$y = [1 + G_n(s)]\alpha_0(x) , \tag{40}$$

where

$$G_n(s) \triangleq \frac{s^n[\Delta(s) - 1]}{\Delta(s)\prod_{i=1}^{n}(s + c_i) - s^n[\Delta(s) - 1]} . \tag{41}$$

Thus, the closed-loop system is again depicted in Figure 1 but with G_n given by (41) replacing G_0.

Theorem 4.1 (Stability Margin of Backstepping with Domination). Under Assumptions 1 and 2, the closed-loop system of Figure 1, with G_n given by (41) replacing G_0, and nonlinear damping α_0 given in (3), is GAS for all stable G_n satisfying

$$\mathrm{Re}G_n(j\omega) > -1 + \frac{\rho}{k} . \tag{42}$$

Proof. Same as that of Theorem 2.1. □

Thus, in the backstepping design with domination, the admissible region for the Nyquist plot of G_n given by (41) is the same as that for G_0 in the x-subsystem (13). However, G_n is a function of the original unmodeled dynamics Δ that changes with the number of steps. Here again, since $\Delta(0) \neq 0$, the starting point of the Nyquist plot of G_n is the origin, if Δ is strictly proper its final point is -1.

As before, we consider separately the cases of ρ positive and negative.

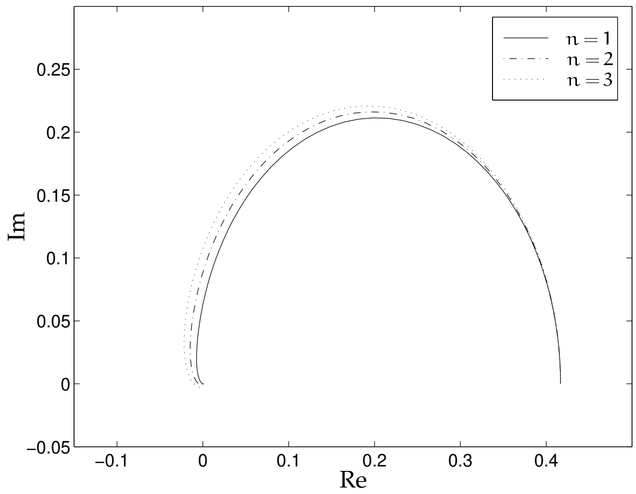

Figure 10: Nyquist plot of $[1-\Delta^{-1}]P_n$, $n = 1,2,3$, for $\Delta(s) = \frac{12(s+35)(s+20)}{7(s+40)(s+30)}$ with $c_1 = c_2 = c_3 = 0.5$.

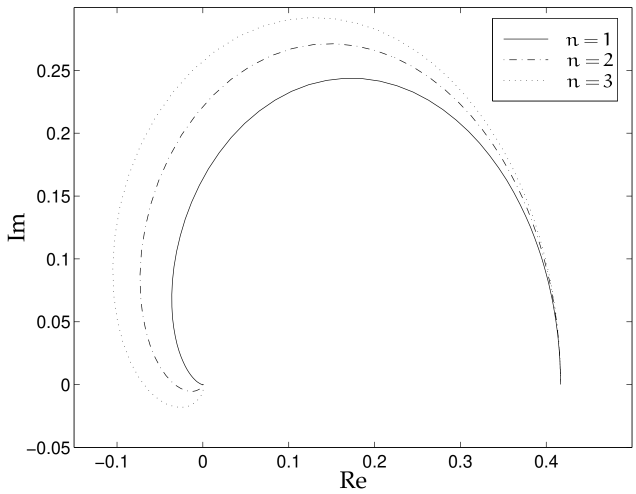

Figure 11: Nyquist plot of $[1-\Delta^{-1}]P_n$, $n = 1,2,3$, for $\Delta(s) = \frac{12(s+35)(s+20)}{7(s+40)(s+30)}$ and three with $c_1 = c_2 = c_3 = 5$.

We observe that $\rho < 0$ in Assumption 1 implies that

$$L_f V(x) + \frac{|\rho|}{2}(L_g V)^2(x) + \frac{|\rho|}{2} h(x)^2 \leq 0 ,$$

where $h(x) = L_g V(x)$. Thus, the x subsystem $\dot{x} = f(x) + g(x)y$ has finite L_2-gain from the input y to the output $h(x)$ (van der Schaft 1992).

5 Conclusions

Our analysis has characterized linear input unmodeled dynamics for which backstepping designs preserve GAS. In particular, GAS will be preserved with *strictly proper* unmodeled dynamics if the open-loop system satisfies the growth condition (2) with $\rho < 0$, that is, if it has finite L_2-gain for the output $L_g V$. If the open-loop system is unstable and satisfies (2) with $\rho > 0$, then only *biproper* unmodeled dynamics can be tolerated.

We have qualitatively shown that with a choice of design parameters an improvement in the stability margins can be traded off with closed-loop performance.

An important implication of our results is that the backstepping design with domination tolerates a larger class of unmodeled dynamics than the backstepping design with cancelation.

Acknowledgment. We thank Mrdjan Jancović, Murat Arcak and Anders Rantzer for very helpful discussions during the development of these results.

References

Hill, D. & Moylan, P. (1976), 'The stability of nonlinear dissipative systems', *IEEE Trans. Automat. Contr.* **21**(5), 708–711.

Hill, D. & Moylan, P. (1977), 'Stability results for nonlinear feedback systems', *Automatica* **13**, 377–382.

Jiang, Z. & Mareels, I. (1997), 'A small-gain control method for nonlinear cascaded systems with dynamic uncertainties', *IEEE Trans. Automat. Contr.* **42**(3), 292–308.

Jiang, Z., Mareels, I. & Pomet, J. (1996), Controlling nonlinear systems with input unmodeled dynamics, *in* 'Proceedings of the 35th CDC', Kobe, Japan, pp. 805–806.

Jurdjevic, V. & Quinn, J. (1978), 'Controllability and stability', *J. Differential Equations* **28**, 381–389.

Krstić, M., Kanellakopoulos, I. & Kokotović, P. (1995), *Nonlinear and adaptive control design*, John Wiley & Sons.

Krstić, M., Sun, J. & Kokotović, P. (1996), 'Robust control of nonlinear systems with input unmodeled dynamics', *IEEE Trans. Automat. Contr.* **41**(6), 913–920.

Megretski, A. & Rantzer, A. (1997), 'System analysis via integral quadratic constraints', *IEEE Trans. Automat. Contr.* **42**(6), 819–830.

Praly, L. & Wang, Y. (1996), 'Stabilization in spite of matched unmodeled dynamics and an equivalent definition of input-to-state stability', *Math. Contr., Signals, Syst.* **9**, 1–33.

Sepulchre, R., Janković, M. & Kokotović, P. (1997), *Constructive Nonlinear Control*, CCES Series, Springer-Verlag.

van der Schaft, A. (1992), 'L_2-gain analysis of nonlinear systems and nonlinear state feedback H_∞ control', *IEEE Trans. Automat. Contr.* **37**(6), 770–784.

Willems, J. (1972), 'Dissipative dynamical systems. Part I: General theory. Part II: Linear systems with quadratic suply rates', *Arch. Rational Mechanics and Analisys* **vol. 45**(Nr. 5), pp. 321–393.